MODELLING TUNA PURSE SEINERS FUEL EFFICIENCY IN REAL-WORLD OPERATIONS USING MACHINE LEARNING APPROACHES

Yi Zhou[1], Kayvan Pazouki[1], Alan J. Murphy[1], Zigor Uriondo[2], Igor Granado[3], Iñaki Quincoces[3], Jose A. Fernandes-Salvador[3]
[1] School of Engineering, Newcastle University, Newcastle upon Tyne, UK
[2] Department of Thermal Engineering, University of the Basque Country UPV/EHU, Spain
[3] AZTI, Marine Research, Basque Research and Technology Alliance (BRTA), Spain

Abstract. Accurate and reliable predictions of ship operating fuel expenditures can significantly increase the ship's operation environmental sustainability and profitability. Given there are general aims of shipping economically and reducing greenhouse gas (GHG) emissions worldwide, fuel consumption needs to be reduced to mitigate operational costs and GHG emissions. Improvement of operational strategies through accurately attributing ship fuel consumption rates to relevant ship operating modes is a way of achieving these aims. This, however, is difficult because the state of the vessel and its machinery systems are not constant (e.g., fouling extent and engine condition). Moreover, the state of the environment (currents, waves and winds) is also not constant. One commercial example where this challenge is particularly acute is in the case of distant fleet fishing operations, where fuel consumption often represents 50% or more of the total operational costs. In this industry there is a demand to develop a decision support system for optimal routing and planning. In this paper, these fishing operations are used to demonstrate a comparison of multiple regression algorithms for a fishing ship's fuel oil consumption prediction model based on two in-situ vessel monitoring systems and environmental conditions forecast from public sources. Based on these data, the Correlation-based Feature Selection (CFS) method is carried out to select the best subset of predictive variables. Multiple regression algorithms are developed and applied, including Linear Regression, Random Forest, XGBoost and Neural Network with the result of Random Forest outperforming the rest of the algorithms for the two fishing vessels. The final selected models show accuracies of over 90% in all the speeds greater than 4 knots when the vessel is not in fishing-related operations but searching for fishing grounds, which accounts for over 90% of the total fuel consumption. From the sensitivity tests carried out on the developed models, it was found that ship speed through water is the variable with critical importance for predicting fuel consumption in both engine operating modes, which contributes to over 94.20% deviation to the baseline in kilograms per nautical mile, followed by month after last drydock (up to 4.34%) and environmental variables (up to 3.30%). This paper considers the practicalities of dealing with the complex data aggregation process from the two distinctly different sources, and demonstrates the relative performance merits of the different algorithms according to key indicators, such as the custom accuracy and the mean absolute error (MAE).

Keywords: FOC prediction, Ship energy efficiency, Multiple regression, Machine learning, Route Optimization.

Recommended citation:
Zhou, Y., Pazouki, K., Murphy, A.J., Uriondo, Z., Granado, I., Quincoces, I., Fernandes-Salvador, J.A. (2022). Modelling tuna purse seiners fuel efficiency in real-world operations using machine learning approaches. In: Proceedings of 15th International Symposium on Practical Design of Ships and Other Floating Structures (PRADS 2022) (eds. Vladimir, N., Malenica, S., Senjanovic, I.). ISBN 978-953-7738-87-7. 9-13 October 2022, Dubrovnik, Croatia. Pp 1410-1426. https://www.doi.org/10.5281/zenodo.7533412

* *Correspondence to: Yi.Zhou2@newcastle.ac.uk*

1. Introduction

Recently, the International Maritime Organization (IMO) introduced long-term strategies reacting to European directives to reduce the environmental footprint of maritime operations. To that end, the maritime industry will have to reduce its carbon intensity by at least 40% by 2030 and try to achieve 70% reductions by 2050. Furthermore, the total annual greenhouse gas (GHG) emissions from international shipping must be reduced by at least 50% by 2050, compared to the data in 2008 [1]. It has been emphasised in the relevant literature that currently available mitigation measures to reduce ships' emissions are critical to achieve the global goals set by the Paris Agreement [2]. Together with the emission reduction issues related to environmental benefits, saving in operating costs is another reason for investigating mitigation solutions for ship emissions. Route optimization is one of the measures to increase the efficiency of operation, which can lead to a reduction of operating costs, thus an increase in profitability [3]. It has been justified in previous research that weather routing can achieve a 2–4 % reduction in fuel consumption and associated GHG emissions [4]. Thus, identifying optimal shipping routes taking the weather conditions into consideration can significantly contribute to the reduction in operational costs and GHG emissions. For fishery activities, this saving in operational costs could be even more important as fuel consumption amounts to a large proportion of total costs [5]. Inefficient fishing activities have resulted in large quantities of fuel being consumed while searching for fish, which definitely increase the emissions and overall costs.

Generally, the framework for a Fishery Route Optimization Decision Support System (FRODSS) can be defined by five layers [6]: i) Environmental layer; ii) Fisheries layer; iii) Ship modelling layer; iv) Routing and planning layer; and v) Decision layer. This study will mainly focus on the environmental and ship modelling layers. The environmental layer provides the ocean information needed to model the ship's behaviour under different weather conditions, where the significant weather variables, such as waves, wind and currents, are identified and taken into consideration. Once this layer is defined, the ship modelling layer identifies and predicts ship performance under different weather conditions in any possible future routes, which will provide the necessary inputs for the two final layers: the route and planning layer and the decision layer. The complexity of this prediction is almost apparent, as it is based on highly stochastic processes which introduce a series of uncertainties in the results [7]. Moreover, such prediction is crucial for FRODSSs that have an additional layer of searching for fish [6] since this searching represents over 90% of the fuel consumption in tuna purse seiners [8].

Recently, many researchers have been contributing to data-driven methodologies relevant to fuel efficiency and Fuel Oil Consumption (FOC) modelling. Petersen et al. [9] evaluated the engine performance of a ferry based on main engine FOC modelling approaches. An Artificial Neural Network model was implemented in their research to estimate fuel consumption and speed through water based on predictors such as draught, trim, port and starboard pitch, port and starboard rudder, heel, port and starboard level and wind effects. The output from the derived models has been used for trim optimization purposes. Beşikçi et al. [10] developed machine learning models such as shallow Artificial Neural Network (ANN) and Multiple Regression (MR) models for the prediction of ship FOC in multiple operating conditions of an oil tanker. They found that the ANN model yielded better performance when compared to the MR model. Similar to the purpose of this work, the model has been applied as a basis for a decision-making system. However, in the work of Wang et al. [11], it has been justified that the Least Absolute Shrinkage and Selection Operator (LASSO) regression model for the estimation of a vessel's FOC had better performance when compared to ANN, Support Vector Regressor (SVR), and Gaussian Processes (GPs) models in their case where the datasets were derived from a container ship. Coraddu et al. [12] provided an investigation on the problems of predicting the fuel consumption and providing the best value for the trim of a vessel in real operations based on data from onboard automation systems by applying white, grey, and black box models for FOC prediction. In their research, it was found that a grey box model can be used as an effective tool for optimizing the trim and forecasting FOC of a tanker in real operational conditions. Gkerekos et al. [3] conducted a comprehensive examination of data-driven modelling approaches, including various multiple regression algorithms: Support Vector Machines (SVMs), Random Forest Regressors (RFRs), Extra Trees Regressors (ETRs), Artificial Neural Networks (ANNs), and ensemble methods to identify the efficacy of different models in modelling vessel FOC consumption from two different shipboard data sources, noon-reports and Automated Data Logging & Monitoring (ADLM) systems. They found that ETRs, RFRs, SVRs, and ANNs yielded the best performance results for both datasets of the target vessel. In the research of Uyanık et al. [13], various prediction models such as Multiple Linear Regression (MLR), Ridge and LASSO Regression, Support Vector Regression (SVR), Tree-Based Algorithms and Boosting Algorithms have been established for a container ship. The predictors in their research were mainly obtained from main engine parameters, such as engine power, temperature and pressure variables. They have concluded that with the proposed methodology in their work, both purposes of route optimization and engine fault detection can be achieved. For more recent work, Papandreou and Ziakopoulos [14] have retrieved data from Very Large Crude Oil Carriers (VLCC). Multivariate Polynomial Regression (MPR), Artificial Neural Networks (ANNs) and eXtreme Gradient Boosting (XGBoost) regression

models were developed and compared according to their performance in fuel consumption prediction. They found that XGBoost had the best performance over other models in terms of model performance and cost of time.

From the published research presented above, it can be concluded that many researchers have been focusing on the estimation and forecasting of vessels' FOC in recent years, with multiple different approaches being implemented. However, most of this research is conducted based on in-situ measured environmental data, few of it was carried out based on open-source data sources that provide several days' forecast for DSSs planning, and none applied to fishing vessels. Previous research has shown that Automated Data Logging & Monitoring (ADLM) systems and noon-reports can be used for data collection, but these data sources are not always available due to the high costs of installing in-situ sensors. In addition, using predictable variables is especially significant for route optimization in fishing vessels. Moreover, none of the reviewed studies model and forecast the operational FOC of a fishing vessel, where it is important to consider the vessel type and fishing gear since their FOC can vary from 1.94 L/mile to 74.2 L/mile [8]. This is basically because targeted fish schools change their distribution over time, increasing the fuel consumption when locating and heading for the fishing grounds [8]. Identifying the weather conditions in advance will significantly contribute to the precise fuel modelling of possible future voyages.

In this work, both in situ data measured by sensors on board two fishery vessels and environmental data from Copernicus' Marine Environment Monitoring Service and NOAA's Global Forecast System are retrieved and processed for fuel consumption modelling and forecasting. Machine learning methods, namely Multiple Linear Regression (MLR), Random Forest (RF), XGBoost (Xg) and Deep Neural Networks (DNN), are employed to forecast fuel consumption considering weather conditions. This forecast is needed to select the best among all the possible routes available in the routing and planning and decision layers of FRODSS. The developed models are then compared according to their cross-validation results and statistically tested to select the model with superior performance. Finally, a future unseen test set is applied to examine the precision of the selected model when new seasonal data is available.

The remainder of this article is outlined as follows: **Section 2** elaborates on the methodology, comprising an overview of the mathematical background of the implemented methods, as well as data collection and processing strategies. A cross-validation strategy and statistical tests are then introduced to select the model with the best performance. Model evaluation metrics are also presented in this section. **Section 3** provides the model performance and selection based on the cross-validation stage with statistical tests. The selected models are then evaluated against unknown test sets in different ship operating modes. The analysis and discussion with regard to the results are also elaborated. Finally, in **Section 4**, overall conclusions and potential future work are provided.

2. Methodological approach

2.1. Data acquisition

Data in this research have been collected from both onboard sensors and open-source environmental datasets:

1) The in-situ data used in this work have been retrieved from onboard sensors of two twin tropical tuna purse seine ships (Ship E. and Ship J.) from the same tuna fishing company, under the same technical specifications. The onboard sensors and data measuring systems were connected to a signal processing and automatic retrieving and storing system called Ratatosk [15] through Ethernet and Modbus. The data collected by Ratatosk are stored on board and periodically synchronized to the onshore servers and stored in NetCDF format. Initial data cleaning and filtering methods have been equipped in the batching processing stage of NetCDF file processing. With the proposed approach, the NaN samples, missing features and unrealistic data would be eliminated during the process of converting the NetCDF files to CSV for visualization.

2) The most significant external factors affecting the vessel's performance and fuel consumption are those related to the weather (waves, wind and currents). Therefore, a model to forecast the vessel's fuel consumption needs to consider these variables and their effect on the ship's speed and fuel consumption. These data have been collected from Copernicus' Marine Environment Monitoring Service (CMEMS), which provides predictions on the physical state of the ocean, variability and dynamics across the globe, and NOAA's Global Forecast System (GFS), which provides wind forecasts. Here, the following short-term forecast products were used: 1) CMEMS Global Ocean 1/12° Physics Analysis and Forecast updated Daily (PHY) [16], which provides currents related data, 2) CMEMS Global Ocean Waves Analysis and Forecast (WAV) [17], which offers wave related data, 3) NOAA GFS 0.25 degree resolution [18], which provides wind data. CMEMS provides user interfaces for extracting data in specific areas and time periods. For PHY Data, the product has a spatial resolution of 0.083° × 0.083° (1/12 degree or 5 minutes). For time averaging, it offers hourly mean data of the variables (centred every half-hour). For WAV data, its spatial resolution is the same as PHY Data, but the temporal resolution is every 3 hours. On the other hand, wind data derived from GFS are provided every 6 hours, with a spatial resolution of 0.25° × 0.25°. The wind data from CMEMS is not considered in this research as CMEMS only provides wind data from observations, not a modelled forecast of Global Surface Winds as NOAA's GFS does.

2.2. Vessel data pre-processing

Automated sensors and Ratatosk installed onboard ensure data recording and integration. However, various issues may arise in terms of accuracy, variations, signal noise and calibration necessity. Proper data cleaning and filtering steps must be taken to ensure that only reliable data remain in the dataset. For the considered datasets, erroneous data (NaN, unrealistic values, etc.) were initially removed by a batch process method. Additional filters are required to identify outliers or physical impossibilities. One approach for identifying outliers in the data is implemented and demonstrated below [19]:

$$x_i = \begin{cases} outlier, if\ |x_i - \mu| > 3\sigma \\ normal, otherwise \end{cases} \quad (1)$$

where x_i represents the i-th observed data point, μ is the mean of all observed data, and σ is the standard deviation. Assuming a normal distribution, 99.7% of normal data should be within $\mu \pm 3\sigma$. This formulation filters out erroneous data points from the dataset. An additional step in the pre-processing stage of a high frequency data set is to smooth the response of signals to capture the important patterns in data while leaving out noise, with the aim of: 1) Matching the frequency of environmental data; and 2) Smoothing noise from the averaging method. An example of the averaged versus the original signal based on Ship J.'s dataset is demonstrated in the left panel of Figure 1, whereas the right panel shows the operating range of speed through water (STW) for the two vessels in Aug. 2021, where travelling at speeds under 4 knots was identified with starting fishing operations. It highlights that the continuous operating range for STW is within 12 to 16 knots while searching and reaching fishing grounds.

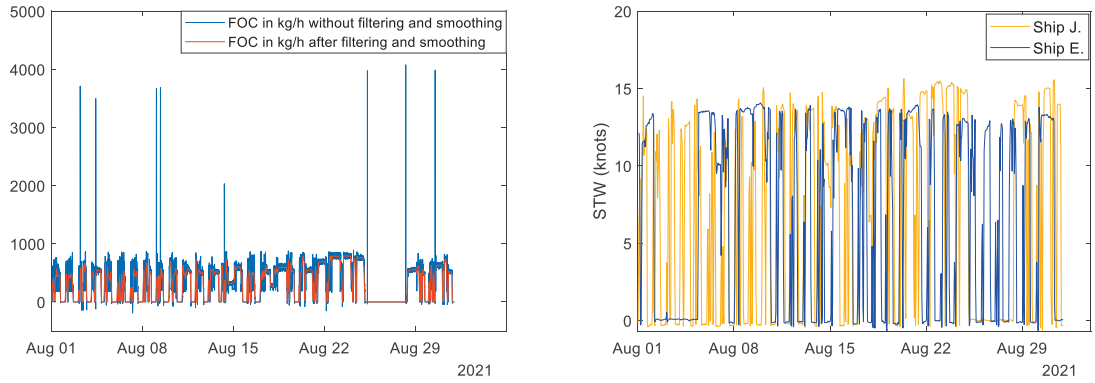

Figure 1. FOC samples of one vessel plotted on its original form (blue line) and after being smoothed (red line) in 1-hour averaging time windows over one month (left panel). Ship E. and J. STW ranges in Aug. 2021(right panel).

In order to match the time averaging strategy of the collected environmental data, the ships' in-situ data has been aggregated hourly. The weather data of a specific area provided by CMEMS and GFS are related to each ship's position (longitude and latitude) and its date and time. Thus, to extract the data according to the ship's location, date and time, the ship's data must fit the three indexes from the environmental data sources. The Nearest Neighbours Imputation method proposed by Faisal and Tutz [20] is applied to find the 1st nearest neighbouring indexes for environmental data selection. Weather data following a space-fixed frame of reference are either provided in the form of a northward and eastward component or in that of a magnitude and an angle. To take the ship's heading into consideration, these measurements are transformed into a body-fixed frame of reference. In the case where the measurements are described by a magnitude M and an angle α, the variables can be transformed into the vessel's body-fixed frame of reference sailing at a heading (hdt), obtaining the longitudinal (lg) and transverse (tr) components by applying the following formulas [21]:

$$lg = M \cdot cos(\alpha - hdt) \tag{2}$$

$$tr = |M \cdot sin(\alpha - hdt)| \tag{3}$$

To transform the measurements that are provided in a northward (nw) and eastward (ew) component into the vessel's body-fixed frame, the following formulas can be used [21]:

$$lg = nw \cdot \cos(hdt) + ew \cdot sin(hdt) \tag{4}$$

$$tr = |ew \cdot \cos(hdt)| + nw \cdot sin(hdt) \tag{5}$$

2.3. Feature selection strategy and standardization

The aim of this work is to develop a model to forecast the vessel's fuel consumption within a few hours or days for route optimization purposes. Therefore, only the predictable in-situ and environmental variables were used for the modelling. For in-situ data, ship speed through water (STW), defined as the speed of the vessel relative to the water, is selected as one of the predictors as it is more accurate predicting fuel consumption than Speed Over Ground (SOG), which is the speed of the vessel relative to the surface of the earth, and it is a good proxy of the engine regime [22]. Furthermore, SOG has a greater currents bias than STW. Another important variable is the so-called docking time, which represents the number of months since the hull was last cleaned. This variable is important in the fuel consumption modelling as it potentially represents biological fouling on the hull, which could result in an increase in the added resistance and a deterioration in the propeller's performance, thus a loss in energy efficiency. Apart from the STW, engine speed in terms of revolutions per minute (RPM) mode is also considered as another factor. Both vessels are equipped with a Controllable Pitch Propeller (CPP) system and use both *constant RPM* mode (fixed engine RPM with variable propeller pitch) and *variable RPM* mode (changing engine RPM and propeller pitch in a pre-programmed ratio), where the variable RPM mode is applied in most of the operating time in transit mode (over 90% of operating time), and constant RPM mode is applied mainly in fishing events (over 90% of operating time).

The multivariate Correlation-based Feature Selection (CFS) method [23], for predictors selection, has been adopted to select the non-redundant environment variables with higher predictive power. The CFS formulation is

based upon the assumption that a good subset of predictors (features in the data mining literature) is one that is highly correlated with the fuel consumption, and at the same time, the predictors have low correlation between them. This reduces the amount of data to download, storage and process while keeping the highest predictive performance. Correlation between two variables is calculated by means of Pearson's Correlation Coefficient during the CFS.

Before model training, standardization is implemented to the predictors of the datasets, which is a process involving mathematical adjustments to produce datasets where all variables have normalized ranges. This process has been executed in ML practices to gain faster computational speeds and convergence [24]. In this study, the z-score normalization was applied. For each variable, x_i, the mean, μ_i, and standard deviation, σ_i, were calculated. Each standardized variable, $x_{standardized}$, can be obtained from the equation below:

$$x_{standardized} = \frac{x_i - \mu_i}{\sigma_i} \tag{6}$$

This method is also known as scaler, where the above relation is retained from the training dataset and used for the scaling of validation and testing datasets afterwards. This transfer occurs so that new data do not require new information to be scaled, to avoid the risk of inferring unseen test data.

2.4. Modelling methodologies

More recently, machine learning regression approaches have been widely used in data-driven fuel modelling. Regression models can be derived with a level of complexity and consequently accuracy of results. Therefore, possible methods and algorithms span a wide range of selections, from multiple linear models [3] to neural network and tree-based methods [14], among which the most promising algorithms are Random Forest, XGBoost and Neural Networks. These three modelling methodologies will be introduced in the next section. Multiple Linear Regression will also be implemented as a baseline against the performance of other models.

Multiple Linear Regression (MLR) is a parametric model, which has been considered as the simplest regression algorithm. Assuming the input variables $x_i = (x_i, \ldots, x_K)$, the predicted target value is then expressed as [25]:

$$y(x_i, w) = w_0 + w_1 x_1 + \cdots + w_K x_K \tag{7}$$

The weight w_j, $j = (0, \ldots, K)$ can be calculated through the Least Squares method:

$$\hat{w} = argmin_w \left\{ \sum_{i=1}^{N} (y_i - w_0 - \sum_{j=1}^{K} (w_j x_{ij})) \right\}^2 \tag{8}$$

Multiple decision trees grow in Random Forest (RF) regression and integrate to achieve a more accurate and stable prediction. This structure is shown in Figure 2 [13]. It gives results in a discrete manner since the decision is based on trees. The RF on this regression model is developed based on the bagging method, by which new trees are created by taking samples in multiple epochs in the sample data set and RF is extracted from these trees.

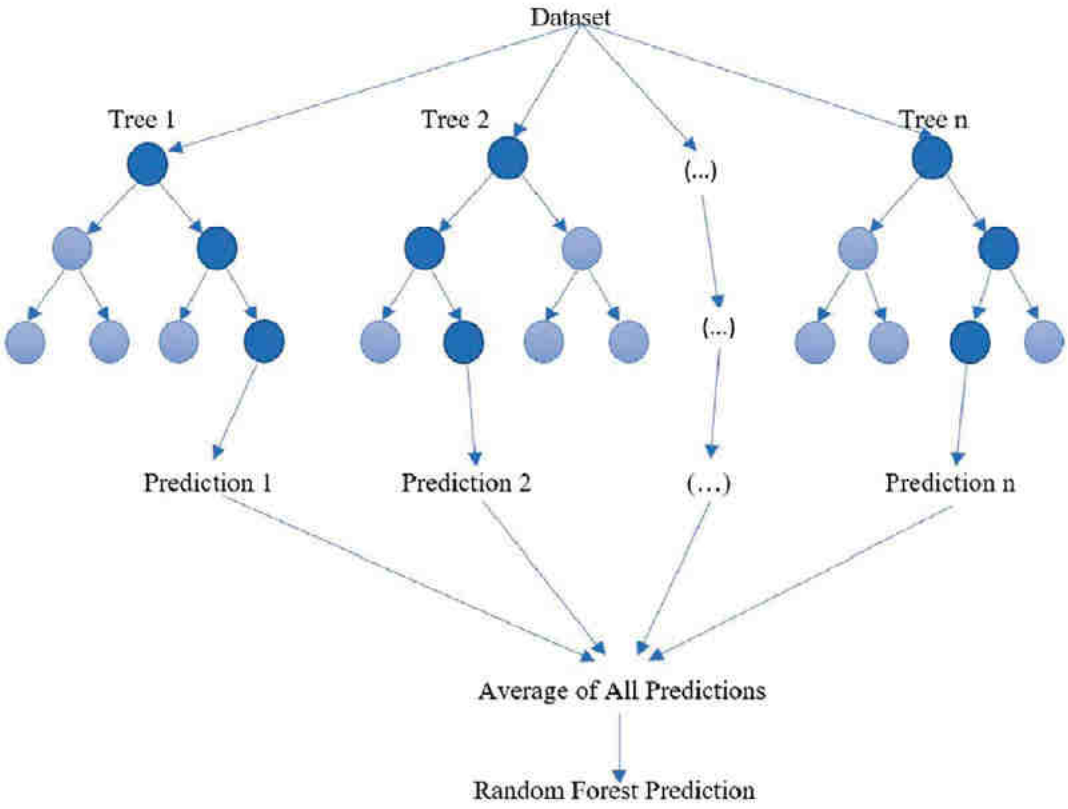

Figure 2. Random Forest Regression

XGBoost (Xg) regression is a supervised ML technique that consists of multiple classification and regression trees. A more detailed overview of the algorithm is introduced in Chen and Guestrin [26]. To summarize their findings, assuming that there is a mapping function between variables:

$$y_{prediction} = f(x_i), \tag{9}$$

where y is the target variable, $y_{prediction}$ is the predicted value of the variable and x_i are the predictors in *i* samples. The tree ensemble model applies a number of functions K to predict y:

$$y_{prediction} = \varphi(x_i) = \sum_{k=1}^{K} f(x_i) \tag{10}$$

Then a loss function is defined according to $y_{prediction\,i}$ and true value y_i for a set of parameters φ_i as $l(\varphi_i)$. Together with the penalizing term for model complexity $\tau(f)$, the objective function can be formulated as:

$$L(\varphi_i)=\sum_{i=1}^{I} l(\, y_{prediction\,i}, y_i) + \sum_{k=1}^{K} \tau(f) \tag{11}$$

The XGBoost model is then trained to minimize the objective function.

The basic working principle of an ANN method is: given an ANN regressor with an input layer **x**, a hidden layer with *M* nodes Z_m, and a single output layer, in each node, the transfer function can be expressed as [27]:

$$Z_m = \sigma(\, \alpha_{0m} + \alpha_m^T x) \tag{12}$$

$$Y = f(x) = g(\, w_0 + w^T Z), \tag{13}$$

where $Z = (Z_1, Z_2, \ldots\ldots Z_m)$, $\sigma()$ is the activation function and $g()$ is the output function. In regression tasks, the output function is usually the identity function. The above transfer function can be implemented for the case

of various layer conditions by passing the output of each layer to the next. The weight parameters α and w are often tuned to get the optimal hyperparameter set.

2.5. Model evaluation metrics

The key indicator of model evaluation in this work (cross-validation and test stages) is Mean Absolute Error (MAE), which can be expressed as [14]:

$$MAE(y_i, \hat{y}_i) = \frac{1}{n}\sum_{i=1}^{n}|y_i - \hat{y}_i| \quad (14)$$

where n is the number of samples in y, $\hat{y}_i$ is the prediction by model, and y_i is the true value. $|y_i - \hat{y}_i|$ is then the absolute error (AE) over n samples. Moreover, for a regression model, a major difficulty of accuracy evaluation is that it becomes numerically unstable when there exists y_i=0. In order to overcome the problem, the custom accuracy applied in this study is expressed as:

$$Custom\ Accuracy = \begin{cases} 100\% - \frac{1}{n}\sum_{i=1}^{n}\left|\frac{y_i - \hat{y}_i}{y_i}\right| \cdot 100\%, if\ y_i > 0 \\ Sample\ removed, otherwise \end{cases} \quad (15)$$

where the accuracy of each sample is $Acc = 100\% - \left|\frac{y_i - \hat{y}_i}{y_i}\right| \cdot 100\%$.

2.6. Cross-validation strategy and statistical tests for optimal model selection

In order to reasonably ensure that selected hyperparameter values are actually close to optimal and not merely overfitting the model, 10 times repeated 5-folds cross-validation is applied in this work. Moreover, cross-validation (cv) allows to compare the different models and choose one using a 5x2cv combined F test, which has been considered as one of the most robust statistical test methods [28]. The P-value of each model can be computed during the test and then compared with a previously chosen significance level. Generally, the significant level threshold is set as α=0.05. If the P-value is smaller than α, null hypothesis can be rejected, and it is accepted that there is a significant difference in the two algorithms.

By integrating the proposed Repeated K-Folds Cross-validation strategy and the statistical tests, the overall cross-validation strategy with hyperparameter tuning and statistical test implemented is shown in Figure 3. In total, 50 runs are required for each of the N hyperparameters tested in each of the four model algorithms during the cross-validation stage. The validation metrics (MAE) of the N hyperparameter sets will be compared to select the set with minimal loss to retrain the model and get each type of model with its optimal hyperparameters. Finally, in-total four models with optimal hyperparameters are compared with 5×2 cv F test. For Ship E., data from February 2021 to January 2022 are used as a training/validation set (6356 hourly-based samples) and for Ship J. from June 2021 to January 2022 (2947 hourly-based samples) are used for training/validation. The second vessel's dataset starts in June instead of February due to delays on the monitoring system installation due to COVID and the vessel' availability. A second validation uses February 2022 data in both vessels to assess the model performance over time with new unseen data.

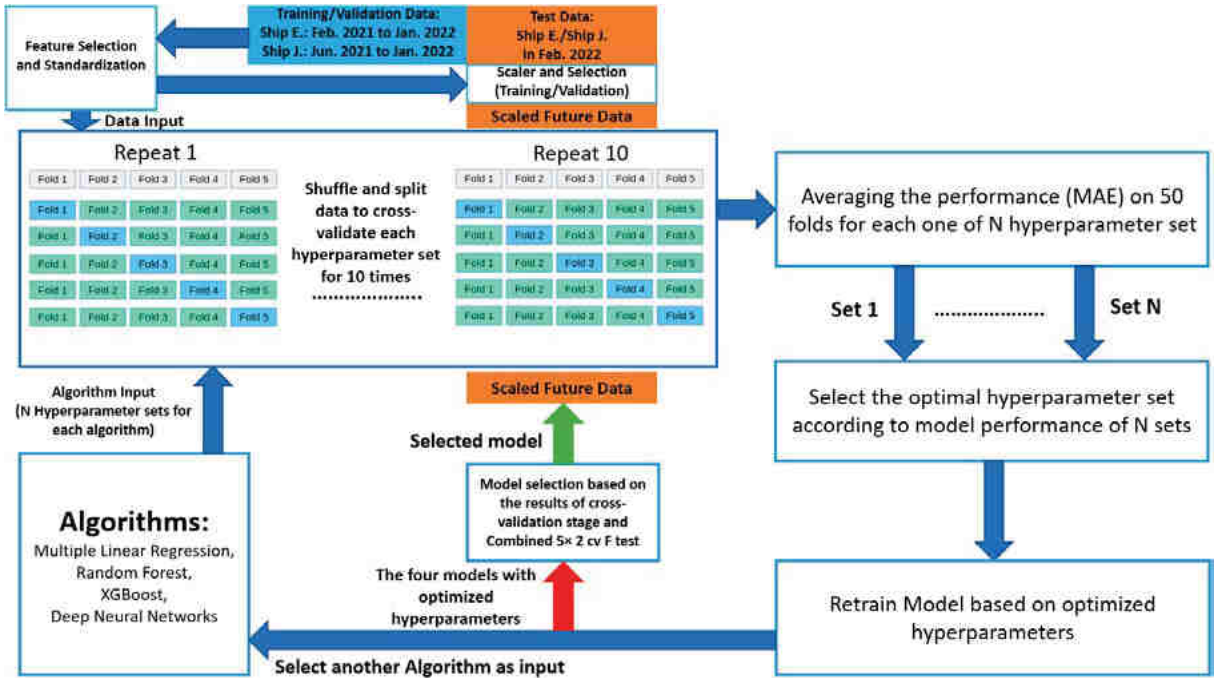

Figure 3. Repeated K-Folds (10 times and 5 folds) Cross-validation strategy with hyperparameter tuning and statistical test implemented.

3. Results and discussion

The final selected features are determined based on the percentage of times they have been selected during the application of CFS in a 10 folds data partition (Freq. Selec. %). The potential predictors, average merit of each selected predictors, and the percentage of times that each predictor has been selected using in 10-fold cross-validation (Freq. Selec. %) are demonstrated in Table 1. Attributes that have been selected over 50% of the times are kept for model training stage.

Table 1. Selection of potential predictors using 10-Folds cross-validation. Data Sources: [i]In-situ, [ii]CMEMS, [iii]GFS

Variable	Average Merit		Freq. Selec. (%)	
	Ship E.	Ship J.	Ship E.	Ship J.
STW[i]	0.991 ± 0	0.991±0	**100 (Selected)**	**100 (Selected)**
VHM0[ii(WAV)]	0.253 ± 0.003	0.271±0.006	0	0
VHM0_SW1[ii(WAV)]	0.218 ± 0.003	0.236 ± 0.006	0	0
VTM01_WW[ii(WAV)]	0.203 ± 0.002	0.232 ± 0.007	0	0
VHM0_SW2[ii(WAV)]	0.202 ± 0.005	0.211 ± 0.009	0	**60 (Selected)**
VHM0_WW[ii(WAV)]	0.188 ± 0.002	0.204 ± 0.006	0	0
t_VHM0_SW2[ii(WAV)]	0.184 ± 0.005	0.195 ± 0.007	0	30
t_VHM0[ii(WAV)]	0.165 ± 0.003	0.054 ± 0.006	0	0
t_VHM0_WW[ii(WAV)]	0.15 ± 0.002	0.098 ± 0.008	0	0
t_VHM0_SW1[ii(WAV)]	0.135 ± 0.004	0.099 ± 0.004	0	0
VSDY[ii(WAV)]	0.083 ± 0.003	0.065 ± 0.004	0	10
VTM10[ii(WAV)]	0.079 ± 0.005	0.011 ± 0.006	0	0
VTM01_SW1[ii(WAV)]	0.065 ± 0.003	0.07 ± 0.007	0	0
VSDX[ii(WAV)]	0.06 ± 0.005	0.023 ± 0.007	**100 (Selected)**	0
l_VHM0_WW[ii(WAV)]	0.054 ± 0.004	-0.057 ± 0.005	0	0
l_VHM0_SW2[ii(WAV)]	0.053 ± 0.005	-0.049 ± 0.006	0	0
VTM02[ii(WAV)]	0.053 ± 0.005	-0.021 ± 0.006	0	0
VTM01_SW2[ii(WAV)]	0.04 ± 0.005	-0.008 ± 0.006	0	0
VTPK[ii(WAV)]	0.024 ± 0.004	-0.003 ± 0.004	0	0
t_o[ii(PHY)]	0.01 ± 0.004	0.157 ± 0.006	0	40
l_tide[ii(PHY)]	0 ± 0.004	-0.002 ± 0.005	0	0
t_VS[ii(WAV)]	-0.002 ± 0.003	0.141 ± 0.007	0	**100 (Selected)**
t_total[ii(PHY)]	-0.005 ± 0.004	0.162 ± 0.007	0	0
l_VHM0[ii(WAV)]	-0.003 ± 0.006	0.014 ± 0.005	0	0
utotal[ii(PHY)]	-0.008 ± 0.004	0.006 ± 0.007	0	0
uo[ii(PHY)]	-0.011 ± 0.004	0.002 ± 0.007	0	0
vtide[ii(PHY)]	-0.018 ± 0.003	-0.028 ± 0.005	0	**70 (Selected)**
vtotal[ii(PHY)]	-0.018 ± 0.004	-0.014 ± 0.005	0	0
utide[ii(PHY)]	-0.026 ± 0.003	0.016 ± 0.005	0	0
l_o[ii(PHY)]	-0.029 ± 0.004	0.082 ± 0.004	0	0
l_VHM0_SW1[ii(WAV)]	-0.031 ± 0.006	0.06 ± 0.005	0	0
vo[ii(PHY)]	-0.033 ± 0.004	-0.022 ± 0.006	0	0
l_total[ii(PHY)]	-0.033 ± 0.004	0.085 ± 0.004	0	50
l_VS[ii(WAV)]	-0.035 ± 0.005	0.053 ± 0.005	**100 (Selected)**	0
l_Wind[iii]	-0.043 ± 0.004	0.042 ± 0.005	0	0
t_Wind[iii]	-0.05 ± 0.003	0.113 ± 0.006	0	0
t_tide[ii(PHY)]	-0.164 ± 0.005	-0.167 ± 0.005	**100 (Selected)**	40

Abbreviation meanings :

VHM0 Significant wave height (m), VTM10 Spectral moments (-1,0) wave period (Tm-10) (s), VTM02 Spectral moments (0,2) wave period (Tm02) (s), VTPK Wave peak period (s), VHM0_WW Spectral significant wind wave height (m), VTM01_WW Spectral moments (0,1) wind wave period (s), VHM0_SW1 Spectral significant primary swell wave height (m), VTM01_SW1 Spectral moments (0,1) primary swell wave period (s), VHM0_SW2 Spectral significant secondary swell wave height (m), VTM01_SW2 Spectral moments (0,1) secondary swell wave period (s), VSDX Eastward Stokes drift U (m/s), VSDY Northward Stokes drift V (m/s), uo Eastward sea water velocity for oceanic general circulation (m/s), vo Northward sea water velocity for oceanic general circulation (m/s), utide Eastward sea water velocity for tide currents (m/s), vtide Northward sea water velocity for tide currents (m/s), utotal Eastward sea water velocity for total currents (m/s), vtotal Northward sea water velocity for total currents (m/s), Wind speed (m/s). l_ and t_: longitudinal and transverse components transformed into the vessel body-fixed frame of reference.

Based on the above discussion and CFS results, the final selected variables are STW, RPM Mode, Month After Last Dry docking, VSDX, l_VS and t_tide for Ship E., and STW, RPM Mode, VHM0_SW2, t_VS and vtide for Ship J. Generally, the environmental features selected are variables related to wave-induced velocity and tide current velocity for the two similar vessels. The discrepancy (Wave height VHM0_SW2 selected for Ship J.) might be associated with the difference in operating routes and strategies. Wind- related variables (speed and direction) were always considered as important factors for fuel consumption prediction in some published research [3][14]. In this research, it is worth noticing that the wind variables are not selected by the proposed feature selection method. Instead, variables related to wave-induced velocity are selected. That is probably because the wind variables are considered as redundant features as it has been proved in previous research that moderately accurate empirical relations exist between the wind speed and the surface wave induced velocity (Stokes drift) [29].

The considered hyperparameter sets for each model and their range of values are presented in Table 2 along with the optimal hyperparameter sets and the optimized losses. From the validation results, it can be deduced that the best performing model was the RF in both datasets. With hyperparameter optimization, it can achieve an average MAE±Std of 11.7±0.5 kg/h and 12.1±0.8 kg/h in Ship E. and Ship J. data sets, respectively, with acceptable training time. XGBoost model also yielded a comparable performance with errors of 12.2±0.4 kg/h and 12.3±0.8 kg/h for the train/validation datasets derived from the two vessels, with a slightly shorter training time when compared to XGBoost. Neural Networks (14.3±0.9 kg/h and 15.3±1.5 kg/h) and Multiple Linear Regression (23.9±0.5 kg/h and 23.4±1.0 kg/h) provide relatively worse performance for both vessels' datasets. In terms of training time, it was observed that training the Neural Networks model required the longest time when compared to the other three models. Although the Multiple Linear Regression model offers the shortest training time, while returns a larger error. The results of the cross-validation for both Ship E. and Ship J., from Table 2 represented as box plots in Figure 4, show that MLR is clearly the model with the worst performance. DNN seems also to perform worse than RF and XG. RF and XG show similar performances and error variance. RF often seems to outperform XG.

Table 2. Model hyperparameters along with their range and validation results. Std: Standard Deviation.

Model	Hyperparameters tuned	Optimal Hyperparameters and Metrics	
		Ship E.	Ship J.
Random Forest	n_estimators∈[200, 2000] max_features∈ ['auto', 'sqrt'] max_depth∈ [10, 110] min_samples_split ∈ [2, 5, 10] min_samples_leaf ∈ [1, 2, 4] bootstrap ∈ [True, False]	bootstrap': True, 'max_depth': 80, 'max_features': 'auto', 'min_samples_leaf': 1, 'min_samples_split': 2, 'n_estimators': 1500, **MAE±Std=11.7±0.5 kg/h**	bootstrap': True, 'max_depth': 105, 'max_features': 'auto', 'min_samples_leaf': 1, 'min_samples_split': 2, 'n_estimators': 1500, **MAE±Std=12.1±0.8 kg/h**
XGBoost	max_depth∈ [2, 10] n_estimators∈[100, 1000] learning_rate ∈ [0.005, 0.01, 0.001]	'learning_rate': 0.01, 'max_depth': 9, 'n_estimators': 850, **MAE±Std=12.2±0.4 kg/h**	'learning_rate': 0.01, 'max_depth': 9, 'n_estimators': 850, **MAE±Std=12.3±0.8 kg/h**
Deep Neural Networks	hidden_layer_sizes∈ [128, 1024; 128, 1024;128, 1024]	activation: RELU hidden_layer_sizes: {'neurons': 1024, 'neurons1': 1024, 'neurons2': 256} **MAE±Std=14.3±0.9 kg/h**	activation: RELU hidden_layer_sizes: {'neurons': 192, 'neurons1': 512, 'neurons2': 128} **MAE±Std=15.3±1.5 kg/h**
Multiple Linear Regression	fit_intercept∈[True, False] normalize∈[Ture, False] positive∈[True, False]	fit_intercept': True 'normalize': Ture 'positive': False **MAE±Std=23.9±0.5 kg/h**	fit_intercept': True 'normalize': Ture 'positive': False **MAE±Std=23.4±1.0 kg/h**

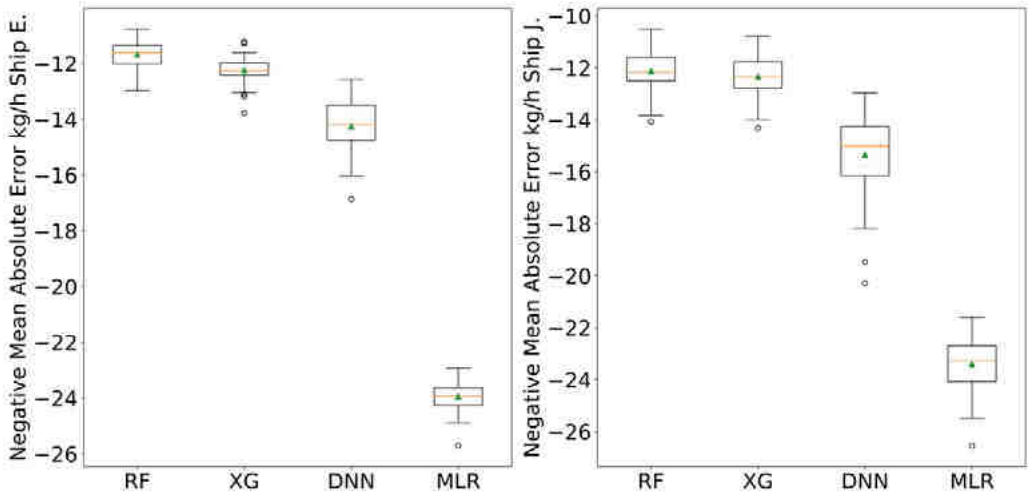

Figure 4. Box plot of the negative MAE obtained from four models' performance with optimal hyperparameters tuned in cross-validation stage

Then the Combined 5×2 cv F test clarifies that RF beats the rest of the algorithms with statistical significance in both vessels' datasets. The results are shown in Table 3, where it can be seen that, for Ship E. and Ship J. datasets, the P-value of each pair model comparison is below 0.05, which means that the null-hypothesis that the four models perform equally well. Thus, it can be concluded that RF yields better performance than XG, DNN and MLR in both ships' datasets according to the results of the cross-validation stage. For most of similar research focusing on the fuel consumption prediction [3][14], the statistical test was not implemented. Since the selection of the models cannot be concluded only from mean performance, this method is required to be implemented to ensure that the difference of mean performance between models is not caused by statistical fluke.

Table 3. Combined 5× 2 cv F test results. * P-value<0.05: Significant, **P-value<0.01 Very Significant

Ship	Model	P-value	f-Statistic
Ship E.	RF vs Xg	0.008**	11.119
	RF vs DNN	0.007**	11.437
	RF vs MLR	6.32e-08**	1338.079
Ship J.	RF vs Xg	0.038*	5.423
	RF vs DNN	0.029*	6.155
	RF vs MLR	1.29e-06**	399.365

Having identified that RF yields less error in terms of MAE at the cross-validation stage, the developed RF models are now evaluated by test datasets (Feb. 2022). As it shown in Figure 5, the models perform well when given the unseen test datasets. The MAEs of the developed RF models on Ship E. and J. test dataset are 14.5 kg/h and 14.3 kg/h, respectively, which are close to the RF model performance derived from cross-validation stage (11.7±0.5 kg/h for Ship E. and 12.1±0.8 for Ship J.). Moreover, it can be roughly deduced that the vessels were mostly working with a main engine fuel consumption rate in the range of 500-700kg/h. This assumption will be clarified and expanded in a further discussion. It is noticed that a limited number of outliers were present in the overall results. These values can be attributed to discrepancies between the actual weather conditions observed in the vessel's ambient space and the environmental data offered by the weather providers [21]. To extend this work, having models based on real vessel sailing data with higher accuracy will be a practical validation of the model's fitness for this purpose.

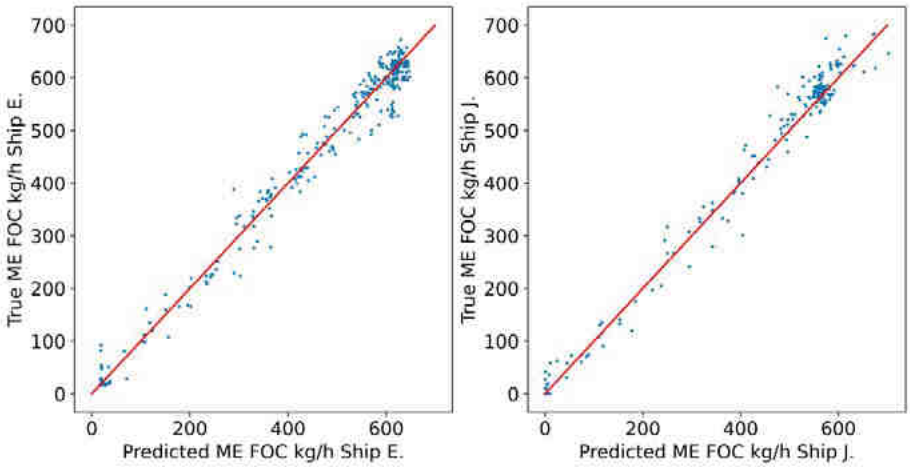

Figure 5. Random Forest model true value by prediction over Ship E. (MAE=14.5kg/h) and J. (MAE=14.3kg/h) test datasets. (True ME FOC: Fuel consumption measurements by flow meters)

For the fisheries route optimization system, the derived FOC model aims to provide a prediction of the vessel's FOC at discretized segments that often span several hours while searching and reaching fishing grounds. Researchers have been focusing on model development under ship transit mode with the vessel speed mostly varying within a small range. Moreover, Table 4 demonstrates that over 60% of total fuel consumption is used in this speed range. Thus, the analysis needs to mainly focus on the samples in this STW range (highlighted in bold in Table 4). Although the MAEs (20.2kg/h for Ship E. and 20.4kg/h for Ship J.) in this speed range are larger when compared with the overall MAEs (14.5kg/h for Ship E. and 14.3kg/h for Ship J.), the errors are calculated in high fuel consumption conditions (average fuel consumption higher than 580kg/h). In this speed range of high consumption, the developed RF models can achieve an accuracy of 96.6% and 96.5%, respectively, with a small standard deviation of 3.6% and 3.0% in sample accuracy to mean accuracy. In terms of the performance of the model in other speed ranges, it was found that the performance of the models is not as accurate as in continuous operating mode. However, the accuracy for the developed RF model can still reach 86.8%, 91.8% and 96.0% in the three speed ranges below 12 knots for Ship E's test dataset, with relatively higher deviation to mean accuracy. In the case of the model performance in Ship J. under various speed ranges shown in Table 4, it is worth noting that the accuracy in the case that STW<4 is quite low. The reason for this is due to the samples with FOC close to 0 (visible in Figure 5, Ship J's case), where minor deviation from true value will lead to a quite large sample percentage error, thus results in a negative accuracy. MAE (5.3kg/h) could be a more reasonable criterion for model performance in this speed range. Nevertheless, it can be inferred from Figure 1 (right panel) that this speed range is not the reference speed during transit. Apart from the case when STW<4, the accuracy for the model goes up to 92.2% and 93.6%, respectively, which indicates that the developed RF models can also provide excellent fuel consumption forecasts during most of the ships' loading conditions.

Besides different loading conditions with ship speed, RPM mode also has an impact on fuel consumption. An indicator that identifies whether the engine system drives propulsion at fixed rpm (constant mode=1) or at variable rpm (variable/combinator mode = -1) has been defined. The choice is made on the basis of the sailing circumstances. In both of the ships, the main operating mode is variable RPM mode with propeller pitch in a pre-programmed ratio, which accounts for a large proportion of total operating time. Overall, the developed RF models yielded a good performance for the voyage in both RPM modes over the two vessels. The model provides high custom accuracy in variable RPM mode (91.5%) and constant RPM mode (96.9%) of Ship E., with standard deviation of 13.7% and 2.3% to mean performance, respectively. In case of Ship J., the CA±Std(Acc) for the model reaches 90.9±17.8% and 89.5±8.4%, in variable RPM mode and constant RPM mode, respectively.

Table 4. Random Forest model performance over different operating modes

Ship E.	Speed Ranges and RPM Modes	Percentage (%) of Time in Each Speed Range and RPM Mode	Actual Accumulated Fuel Consumption (t) and Percentage (%)	MAE (kg/h)	Average Fuel Consumption (kg/h)	CA±Std(Acc)
STW Ranges (knots)	<4	44.6%	8.5(5.3%)	5.4	38.7	86.8±18.3%
	4 to 8	9.3%	17.2(10.8%)	28.2	374	91.8±8.0%
	8 to 12	14.0%	36.7(23.1%)	21.1	532.3	96.0±3.6%
	12 to 16	**32.1%**	**96.5(60.8%)**	**20.2**	**611**	**96.6±3.6%**
RPM Modes	Variable	95.5%	149.7(94.2%)	14.6	318.6	91.5±13.7%
	Constant	4.5%	9.2(5.8%)	12.8	418.5	96.9±2.3%
Ship J.	**Speed Ranges and RPM Modes**	**Percentage (%) of Time in Each Speed Range and RPM Mode**	**Actual Accumulated Fuel Consumption (t) and Percentage (%)**	**MAE (kg/h)**	**Average Fuel Consumption (kg/h)**	**CA±Std(Acc)**
STW Ranges (knots)	<4	46.2%	2.5(2.7%)	5.3	17.1	62.8±33.1%
	4 to 8	5.0%	5.0 (5.4%)	22.0	310.8	92.2±7.5%
	8 to 12	9.2%	13.3(14.2%)	28.4	458.7	93.6±7.0%
	12 to 16	**39.6%**	**72.6(77.7%)**	**20.4**	**580.9**	**96.5±3.0%**
RPM Modes	Variable	98.1%	90.9(97.3%)	13.8	293.2	90.9±17.8%
	Constant	1.9%	2.5((2.7%)	39.1	414.7	89.5±8.4%

To further investigate the impacts of the input in-situ and environmental variables on the fuel consumption rate, a sensitivity analysis similar to [30] has been conducted. Typically, the analysis is conducted by fixing all variables to a constant value and changing a single input variable at a time. As shown in Figure 6, STW is found to be of the most significant variable for predicting fuel consumption in kilogram/nautical mile (kg/nm), which contributes to 94.20% (Ship E.) and 111.61% (Ship J.) deviation over baseline in fuel consumption in kg/nm in variable RPM mode, 231.50% (Ship E.) and 149.80% (Ship J.) deviation to baseline in constant RPM mode, respectively. In both of constant and variable RPM modes, the tendency of fuel consumption variation with increasing STW could be roughly represented by quadratic curves. In terms of the number of months after a dry dock, generally the fuel rate increases the longer the time after the dry dock takes place, which was found to have maximal impact of 2.90% (Ship E.) and 4.34% (Ship J.) on fuel consumption over the baseline. In Ship E., data collection started earlier than Ship J and before going to a second dry dock. In Ship J., data collection started after the dry dock. Thus months 34 to 36 after the first dry dock are included in Ship E's dataset. Taking month 36 after the first dry dock as the model input, the model output fuel consumption rate is 47.25 kg/nm, compared to 45.34 kg/nm when taking month 8 after this dry dock as an input. In terms of the environmental variables, from the groups of diagrams it is suggested that the RF models capture the relationships between the input variables and FOC in an appropriate manner. Moreover, it is found that the impact of these variables on the fuel consumption rate is not as significant as STW in the limited operating area of the two vessels, with the maximal impact from 0.3-3.3% on fuel consumption rate. The cause of the low impacts could be that the skippers of the vessels are always attempting to avoid extreme weather during voyage for fishing, which is also observed from the histograms demonstrating the distribution of variables' deviation. This impact can be justified in the research [4] mentioned in the Introduction, which claimed within 4% FOC reduction could be achieved by weather routing. Although the fuel rate change along with the alteration in the environmental variables is relatively small, a slight decrease in the fuel consumption rate could result in a saving in accumulated fuel consumption. Together with weather routing, a greater than 50 % improvement in ship performance in terms of FOC reduction could be achieved through technical and operational measures such as speed management and fleet planning [31].

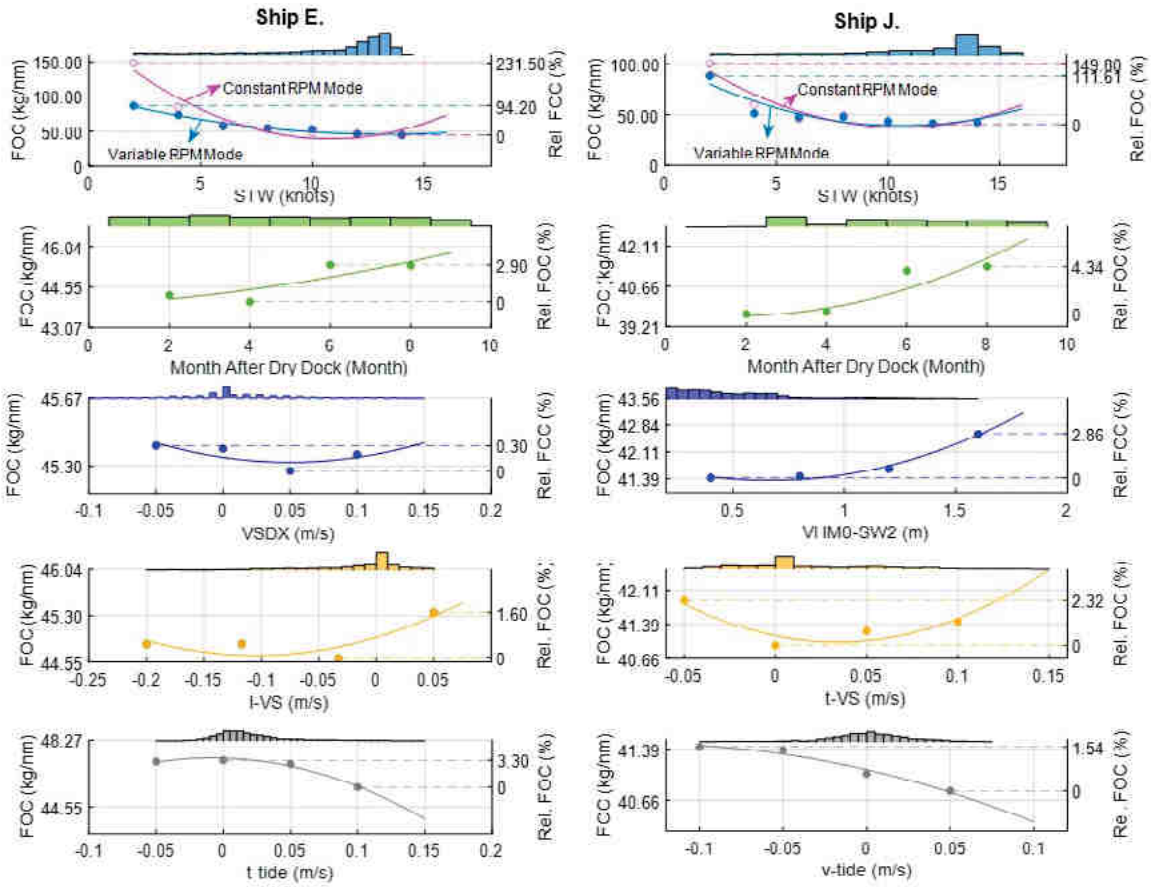

Figure 6. Model Sensitivity Analysis with Histogram Plot of the Attributes. VSDX Eastward Stokes drift. l-VS longitudinal component of Stokes drift in vessel body-fixed frame of reference. t-tide transverse component of tide current in vessel body-fixed frame of reference. VHM0-SW2 Spectral significant secondary swell wave height. t-VS transverse component of Stokes drift in vessel body-fixed frame of reference. v-tide Northward sea water velocity for tide currents.

In summary, there are few studies in the literature that try to optimize the fishing vessels' routes [32][33] and even less considering their FOC according to the weather conditions [6][34][35]. Among the latter, [34][35] only optimize the routes from two known points considering the weather effect on the FOC, but not the search for fish as in [6]. In shipping, there are a lot of studies that optimize the vessels' FOC [36][37][38]; however, it is noteworthy that the fishing vessels' consumption varies according to their characteristics and used fishing gear [5]. Hence, the proposed data-based models, which are vessel specific, give more precise results when modelling the FOC depending on the weather conditions faced by the studied vessels. That is why these models can be integrated in FRODSSs or other weather routing systems to provide a FOC forecast within a few hours or days depending on the weather conditions the vessels are likely to face. These systems can be useful for the fishing industry in order to reduce their footprint and enhance their sustainability.

4. Conclusion and future work

This work aims to provide accurate models that utilize exclusively data from in-situ sensors and weather data from Copernicus' CMEMS service and NOAA's GFS model to model and predict the fuel consumption of fishery ships, which could contribute to the design of a ship route optimization system onboard. Available sensor data and environmental data from two fishing vessels were used in this work. Multiple Linear Regression, Random Forest, XGBoost and Deep Neural Networks models were developed and evaluated based on their loss for predicting fuel consumption in repeated K-folds cross-validation. Moreover, combined 5 × 2 cv F test is applied to check whether the difference of mean performance between models is statistically significant. Finally, the selected models are evaluated against unseen future datasets. The main findings of the research conducted are as follows:

i. Based on the training/validation datasets of the two fishing vessels, a less than 12.1 kg/h MAE was obtained by the optimally performing modelling approach Random Forest through a cross-validation method and hyperparameter optimization.

ii. Combined 5 × 2 cv F test results showed that Random Forest models yield better performance as its lower error at cross-validation stage has been justified to be statistically significant over other algorithms.

iii. The selected Random Forest models can achieve an overall accuracy of over 90% in most operating conditions (STW>4) over the test datasets of the two vessels, which has demonstrated its ability in accurately predicting the FOC of vessels under different weather conditions, ship speed, RPM modes, and biofouling levels. Thus, its superior performance in modelling and predicting fuel consumption for the fishery ships can be justified.

iv. The sensitivity tests have been conducted to test the independent impact on FOC of each selected predictor. It was found that ship speed through water is the variable with most significant impact on fuel consumption, followed by month after dry dock and the selected environmental variables.

This work contributes to the fuel consumption prediction for fishery vessels, while most of similar research focusing on ship fuel consumption prediction is carried out for other types of ships, such as container ships, ferries and oil carriers. In addition, while previously most of the research focusing on ship fuel consumption is conducted based on sensor data measured onboard, in this research the model development was carried out based on predictable in-situ data and open-source data sources that provide several days forecasts, which is more appropriate and reasonable for DSSs planning.

In terms of future work, a lower accuracy of the developed model was detected when STW<4, even if this is not the reference speed range for ship transit. Further investigations are required to address this issue if found relevant for FRODSS. Moreover, for FRODSS development in actual operation conditions, SOG seems to be a more reasonable input as the required system is based on GPS. The relationship between the two speed variables and the impact of weather conditions on this relationship will need to be identified.

5. Acknowledgements

This work has received funding from the European Union's Horizon 2020 research and innovation programme under grant agreement No 869342 (SusTunTech). The authors are grateful to Echebastar for their collaboration in this study. I. G. has been benefited from the IKERTALENT grant of the Department of Economic Development and Infrastructures of the Basque Government.

6. References

[1] International Maritime Organization (IMO). https://www.imo.org/en/ MediaCentre/HotTopics/Pages/Reducing-greenhouse-gas-emissions-from-ships.asp x., 2018.

[2] M. Traut, A. Larkin, K. Anderson, C. McGlade, M. Sharmina, and T. Smith. CO2 abatement goals for international shipping. Climate Policy, vol. 18, no. 8, pp. 1066–1075, Apr. 2018, doi: 10.1080/14693062.2018.1461059.

[3] C. Gkerekos, I. Lazakis, and G. Theotokatos. Machine learning models for predicting ship main engine Fuel Oil Consumption: A comparative study. Ocean Engineering, vol. 188, p. 106282, Sep. 2019, doi: 10.1016/j.oceaneng.2019.106282.

[4] J. Prpić-Oršić, R. Vettor, O. M. Faltinsen, and C. Guedes Soares. The influence of route choice and operating conditions on fuel consumption and CO2 emission of ships. Journal of Marine Science and Technology, vol. 21, no. 3, pp. 434–457, Jan. 2016, doi: 10.1007/s00773-015-0367-5.

[5] O. C. Basurko, G. Gabiña, and Z. Uriondo. Energy performance of fishing vessels and potential savings. Journal of Cleaner Production, vol. 54, pp. 30–40, Sep. 2013, doi: 10.1016/j.jclepro.2013.05.024.

[6] I. Granado, L. Hernando, I. Galparsoro, G. Gabiña, C. Groba, R. Prellezo and J. A. Fernandes. Towards a framework for fishing route optimization decision support systems: Review of the state-of-the-art and challenges. Journal of Cleaner Production, vol. 320, p. 128661, 2021. Available: 10.1016/j.jclepro.2021.128661.

[7] O. Soner, E. Akyuz, and M. Celik. Use of tree based methods in ship performance monitoring under operating conditions. Ocean Engineering, vol. 166, pp. 302–310, 2018.

[8] O. C. Basurko, G. Gabiña, J. Lopez, I. Granado, H. Murua, J.A. Fernandes, I. Krug, J. Ruiz, and Z. Uriondo. Fuel consumption of free-swimming school versus FAD strategies in tropical tuna purse seine fishing. Fish. Res., vol. 245, no. 106139, p. 106139, 2022.

[9] J. P. Petersen, O. Winther, and D. J. Jacobsen. A Machine-Learning Approach to Predict Main Energy Consumption under Realistic Operational Conditions. Ship Technology Research, vol. 59, no. 1, pp. 64–72, Jan. 2012, doi: 10.1179/str.2012.59.1.007.

[10] E. Bal Beşikçi, O. Arslan, O. Turan, and A. I. Ölçer. An artificial neural network based decision support system for energy efficient ship operations. Comput. Oper. Res., vol. 66, pp. 393–401, 2016.

[11] S. Wang, B. Ji, J. Zhao, W. Liu, and T. Xu. Predicting ship fuel consumption based on LASSO regression. Transp. Res. D Transp. Environ., vol. 65, pp. 817–824, 2018.
[12] A. Coraddu, L. Oneto, F. Baldi, and D. Anguita. Vessels fuel consumption forecast and trim optimisation: A data analytics perspective. Ocean Engineering, vol. 130, pp. 351–370, 2017.
[13] T. Uyanık, Ç. Karatuğ, and Y. Arslanoğlu. Machine learning approach to ship fuel consumption: A case of container vessel," Transp. Res. D Transp. Environ., vol. 84, no. 102389, p. 102389, 2020.
[14] C. Papandreou and A. Ziakopoulos. Predicting VLCC fuel consumption with machine learning using operationally available sensor data. Ocean Engineering, vol. 243, no. 110321, p. 110321, 2022.
[15] S. Skjong, L. T. Kyllingstad, K.-J. Reite, J. Haugen, J. Ladstein, and K. G. Aarsæther. Generic on-board decision support system framework for marine operations. In International Conference on Offshore Mechanics and Arctic Engineering, vol. 58844, p. V07AT06A032. American Society of Mechanical Engineers, 2019.
[16] Global Ocean 1/12° Physics Analysis and Forecast updated Daily. https://doi.org/10.48670/moi-00016, 2019.
[17] Global Ocean Waves Analysis and Forecast. https://doi.org/10.48670/moi-00017, 2019.
[18] National Centers for Environmental Prediction/National Weather Service/NOAA/U.S. Department of Commerce. Updated daily. NCEP GFS 0.25 Degree Global Forecast Grids Historical Archive. Research Data Archive at the National Center for Atmospheric Research, Computational and Information Systems Laboratory. https://doi.org/10.5065/D65D8PWK, 2015.
[19] J. F. Hair, W. C. Black, B. J. Babin, R. E. Anderson, and R. L. Tatham. Multivariate Data Analysis: Global Edition. 7th ed. Philadelphia, PA: Pearson Education, 2008.
[20] S. Faisal and G. Tutz. Multiple imputation using nearest neighbor methods. Inf. Sci. (Ny), vol. 570, pp. 500–516, 2021.
[21] C. Gkerekos and I. Lazakis. A novel, data-driven heuristic framework for vessel weather routing. Ocean Engineering, vol. 197, no. 106887, p. 106887, 2020.
[22] P. Gloaguen, M. Woillez, S. Mahévas, Y. Vermard, and E. Rivot. Is speed through water a better proxy for fishing activities than speed over ground?. Aquatic Living Resources, 29(2), p.210, 2016.
[23] M. A. Hall. Correlation-based feature selection of discrete and numeric class machine learning. The University of Waikato, Hamilton, NewZealand, 1999.
[24] S. Ioffe and C. Szegedy. Batch Normalization: Accelerating deep network training by reducing internal covariate shift. In International conference on machine learning, pp. 448-456. PMLR, 2015.
[25] C. M. Bishop. Pattern Recognition and Machine Learning. New York, NY: Springer, 2006.
[26] T. Chen and C. Guestrin. XGBoost: A Scalable Tree Boosting System. In Proceedings of the 22nd acm sigkdd international conference on knowledge discovery and data mining, pp. 785-794. 2016.
[27] T. Hastie, R. Tibshirani, and J. Friedman. The elements of statistical learning: Data mining, inference, and prediction. 2nd edition, 2nd ed. New York, NY: Springer, 2017.
[28] E. Alpaydm, Combined 5 × 2 cv F Test for Comparing Supervised Classification Learning Algorithms. Neural Computation, vol. 11, no. 8, pp. 1885–1892, Nov. 1999, doi: 10.1162/089976699300016007.
[29] T. S. van den Bremer and Ø. Breivik. Stokes drift. Philosophical Transactions of the Royal Society A: Mathematical, Physical and Engineering Sciences, 376(2111), 2018.
[30] S. Washington, M. Karlaftis, F. Mannering and P. Anastasopoulos. Statistical and econometric methods for transportation data analysis. Chapman and Hall/CRC, 2020.
[31] E. H. Green, J. J. Winebrake, and J. Corbett. Prevention of air pollution from ships-Opportunities for reducing greenhouse gas emissions from ships. International Maritime Organization (IMO), Tech. Rep, 2008.
[32] C. Groba, A. Sartal, and X. H.Vázquez. Solving the dynamic traveling salesman problem using a genetic algorithm with trajectory prediction: An application to fish aggregating devices. Computers & Operations Research, 56, pp.22-32, 2015.
[33] C. Groba, A. Sartal, and X. H.Vázquez. Integrating forecasting in metaheuristic methods to solve dynamic routing problems: Evidence from the logistic processes of tuna vessels. Engineering Applications of Artificial Intelligence, 76, pp.55-66, 2018.
[34] G. Mannarini, N. Pinardi, G. Coppini, P. Oddo and A. Iafrati. VISIR-I: small vessels–least-time nautical routes using wave forecasts. Geoscientific Model Development, 9(4), pp.1597-1625, 2016.
[35] R. Vettor & C. G. Soares. Development of a ship weather routing system. Ocean Engineering, 123, 1-14, 2016.
[36] S.-M. Lee, M.-I. Roh, K.-S. Kim, H. Jung, J.J. Park. Method for a simultaneous determination of the path and the speed for ship route planning problems. Ocean Eng. 157, 301–312, 2018. http://dx.doi.org/10.1016/j.oceaneng.2018.03.068.
[37] J. Zheng, H. Zhang, L. Yin, Y. Liang, B. Wang, Z. Li, X. Song, Y. Zhang. A voyage with minimal fuel consumption for cruise ships. J. Clean. Prod. 215,144–153, 2019. http://dx.doi.org/10.1016/j.jclepro.2019.01.032.
[38] K. Takashima, B. Mezaoui, R. Shoji. On the fuel saving operation for coastal merchant ships using weather routing. In: Proceedings of Int. Symp. TransNav, vol.9, pp. 431–436, 2009.